

ISABELLE Project  
BROOKHAVEN NATIONAL LABORATORY  
Associated Universities, Inc.  
Upton, NY 11973

Technical Note No. 365

DIPOLE MAGNET CROSS SECTION MEASUREMENTS

Richard C. Fernow

April 30, 1982

INTRODUCTION

An important consideration related to the ultimate field quality of the dipole magnets is the azimuthal uniformity of the conductor turns. It has been believed for some time that friction during the assembly could cause non-uniform compression particularly with the large inner coil segments. Kapton-teflon slip planes have been introduced in the present dipole magnet design<sup>1</sup> to minimize this problem. However up to now there have been no quantitative measurements of actual turn distributions. In this note we report measurements of the azimuthal uniformity in a compressed cross section of the dipole magnet together with other measurements which are important for field quality. We will also consider the implication of these measurements for the field harmonics.

ASSEMBLY

The yoke for this assembly consisted of two ISA Spec. 3" module halves. The coil sections were cut from curved straight section cured at 10 kpsi. The ends of the cured sections were polished at the Metallurgy division so that the various pieces of the cross section were clearly visible. The coil segments were wrapped with teflon and kapton in the standard ISA manner. G-10 shims were inserted to get the prestress per coil into the usual range. A photograph of the assembled magnet is shown in Fig. 1.

The gap between the yoke halves closed completely at a torque of 225 ft-lbs. The elongation of the stainless steel bolts are shown in Fig. 2 as a function of the applied torque. Due to an unfortunate problem with the yoke key the two yoke halves have a translation along the midplane of 15 mils. The first few inner coil layers closest to the midplane were deformed during the assemblies with the result that several turns have bulged into the aperture by up to 2 mm. It was felt that this phenomenon may be due to the fact that the length of the segment is not much larger than the transposition length of the cable or possibly from an excessive prestress.

<sup>1</sup> R.B. Palmer, et. al., ISABELLE Technical Note No. 320 (1981).

The total force acting on each side can be determined from the bolt elongation to be ~ 25,000 pounds. The distribution of this force between the inner and outer coils estimated from the measurements with the McGahern compression device is 16 kpsi for the AD inner coil arc and around 11 kpsi for the other three coil arcs. However the uncertainty on these numbers is several kpsi.

#### MEASUREMENTS

The x and y coordinates were measured on a Bendix Cordax 803 coordinates measuring machine in Inspection. The device had a least count accuracy of 0.1 mil. The x axis was defined by measuring two points on the midplane between the yoke halves each about 1/2 inches out from the circular aperture. The point x=0 was defined to be the center of the bore tube keyway in the CD pole piece. The coordinates of each point were printed on a paper tape and later punched onto computer cards for analysis.

The actual measurements involved minor difficulties due to chamfer on metal edges. There is a possibility that coil material adjacent to such an edge can flare out into this space. A more significant difficulty at the edges of the coil segments involved the insulation protruding out making it difficult to unambiguously define the edge. It should also be kept in mind that these measurements are only sensitive to conditions on the surface. These may differ from the bulk properties of the magnet particularly since the segments are unconstrained longitudinally.

#### IRON YOKE

Results of 16 measurements along the inner aperture of the yoke are shown in Table I. Two independent measurements of the iron center and radius are given. The center of the iron is clearly offset from the center of the measuring machine. The radius of the AB half agrees very well with the design value of 3.4165 inches but the radius of the CD half is too large by 3 mils.

For field quality studies it is convenient to measure the position of all quantities in a coordinate system centered on the iron yoke. For this purpose a circle is fit thru the measurements of the iron yoke edge. The coordinates of all points are then translated to the iron center coordinates. This is done separately for each yoke half. Then all angles are calculated as the best fit of a straight line from the iron origin thru the measured points. Angles measured in this way typically differ by several tenth of a degree from direct measurements in the machine centered coordinates.

For the purpose of error calculations we have assumed a measurement error of 0.5 mil. We see that the  $\chi^2$  in Table I is quite poor. In Fig. 3 we show the deviations of the measurements in each half from the respective mean radius. It can clearly be seen that outward deformations of order 5 mils occur over a narrow range in the vicinity of 50° from the midplane. We note that this region is near the end of the pole pieces and also corresponds to the polar angle where the iron is thinnest due to the bolt notches.

The displacement of the CD iron center indicates the center of the CD pole piece keyway is asymmetric by  $0.076^\circ$ . Measurements along the yoke mid-planes showed that the angle between them differ from  $180^\circ$  by  $\sim 0.34^\circ$ .

One of the objectives of this study was to identify possible assembly errors that could affect the ultimate field quality of the magnet. Therefore we have examined the changes in multipoles that would be caused if errors of the same magnitude were present in an actual magnet. The resulting figures must be used with caution since, as we have pointed out, these cross section surface measurements are not equivalent to the coil environment in a real magnet. However the exercise is useful in identifying which multipoles are sensitive to the various effects.

Table VI contains the multipoles for the current dipole design evaluated at room temperature. The effect of deformations in the iron yoke near  $45^\circ$  is shown. The effect was approximated by increasing the iron radius by 2 mils for current blocks in the region  $40^\circ < \phi < 60^\circ$  for all quadrants. The coils were kept at the design radii. The change in multipoles is seen to be small. Table VII shows the effect of increasing one of the iron radii by 3 mils and assuming the coils remain at their design radii. The effect of rotating the pole piece by  $0.076^\circ$  is also shown in Table VII. It is assumed that the other pole piece is at the correct position and that the coil segments between the poles expand or compress elastically. Such an effect would produce an appreciable  $b'_1$  term.

#### LAMINATED POLE PIECES

The design geometry of the stainless steel pole pieces is shown in Fig. 4. The design post angles of  $9.41^\circ$  and  $44.24^\circ$  are supposed to be achieved by placing 250 mil rectangular shims between the metal laminations and the coil. Measurements of the effective angle from the iron center to the metal edge are given in Table II. Also given are the distances of closest approach (impact parameter) to the center of the projection of the metal edge. We see that the inner coil angles and impact parameters agree well with the design values. The outer coil angles however are consistently too large by 2-3 mils. This is supported by the impact parameter measurements which are consistently small. Table VI shows the effect of increasing all outer post angles by  $0.065^\circ$ . Such an error could have a significant effect on  $b_2$ .

#### RADIAL UNIFORMITY

The assembly radii predicted from the measured iron radius, measured G-10 cooling channel thickness, and design coil thicknesses are shown in Fig. 5. Actual measurements along the edge of the bare conductor in the outer coil are shown in Fig. 6. The bare conductor width of the cable is about 313 mils. The cable spec. is 308 mils so we see that the conductor has expanded radially. Comparison with the predicted assembly radii in Fig. 5 shows the mean radius of the conductor is about 2 mils further out than expected.

Measurements for the inner coil are shown in Fig. 7. The coil appears relatively uniform up to the region  $45-50^\circ$  where the mean radius appears to increase. The radial extent of the conductor is 8 mils larger than the nominal value of 308 mils. The mean radius for  $0 < \phi < 80^\circ$  is about 14 mils larger than the radii predicted by Fig. 5. In this region the inner coil bears against 3 layers of 10 mil thick G-10 sheets held together with double-sided adhesive. The total insulation between the inside of the outer coil and outside of the inner coil near  $45^\circ$  is only several mils. The effect of systematically using these coil radii in all four quadrants together with the design iron radius is shown in Table VI. Such an effect could significantly alter  $b_2$  and  $b_4$ .

#### G-10 SHIMS

Table III gives the measured sizes of the G-10 shims. Arc lengths are calculated using the measured assembly radii. The observed compression tends to be larger than expected. The stresses calculated from the observed strains are not in agreement with the assumed prestress. However, the shims are very small compared with the coil segments so that a small error in locating the G-10 edge or the longitudinal variation in thickness of the shim can significantly alter the results.

#### COPPER WEDGES

Measurements of the copper wedges size are given in Table IV. The measured thicknesses of the extruded inner wedges are in excellent agreement with the design value. The agreement for the machined outer coil wedges is not so good. This could be due to machining errors or to uncertainty in the actual edge due to chamfer and coil flaring.

#### AZIMUTHAL UNIFORMITY

The measured sizes of the coil segments are given in Table V. For the inner coil the 4 turns near the post consistently have a larger average thickness than the large block of 62 turns nearer the midplane. The compression in the outer coil seems much more uniform. Three of the four segments indicate a small increase in compression near the post.

A plot of the effective angle of a conductor edge versus the turn number for the inner coil is roughly linear. In Fig. 8 we show the deviations of the individual measurements from a straight line fit between the 10th and 62nd turns. Data is shown for two quadrants and for two edges of each conductor in one of the quadrants. The turns appear compressed below turn 20, expanded near turn 40, and probably compressed again near turn 50. The A quadrant points were carefully measured for this purpose and are probably more reliable. We have studied the effect on field quality by approximating the dotted line in Fig. 8 with a series of coil blocks with different average thicknesses. The results shown in Table VI show a significant effect on  $b_2$  and  $b_4$ . In Fig. 9 we give the bare conductor azimuthal thickness. If we neglect the turns closest to the midplane bulge the azimuthal thickness appears to increase away from the midplane. The azimuthal thickness of the insulation shown in Fig. 10 appears to be constant.

The azimuthal uniformity of the outer coil is more uniform. The bare conductor azimuthal thickness shown in Fig. 11 is fairly constant. Again there is a hint of a compression increase near the post. Neglecting the midplane turns the azimuthal thickness of the insulation is fairly constant as shown in Fig. 12.

#### EDGE ANGLE

Ideally the edges of all the keystoneed conductors should point at the center of the magnet. We have checked this by measuring the impact parameter of the projection of each edge to the center of the iron circle fit. This is shown for the inner coil in Fig. 13. Positive impact parameter is defined to be a projection which passes on the coil's side of the origin. We see that the impact parameter peaks near  $30^\circ$  where the angular error is around  $1^\circ$ . The outer coil shown in Fig. 14 appears to be much more uniform.

#### WIRE DENSITY

Finally we have examined the distribution of the 23 wires in the cable. The location of each wire was determined by the small core of pure copper at the center of the wire. The distance  $d$  to the closest neighbor was calculated for each wire. The resulting distribution for four conductors in the C quadrant are shown in Fig. 15. Apart from the usual problem at the midplane the distances tend to grow farther apart as expected except at the outer edge where they tend to be compressed together again.

#### ACKNOWLEDGMENT

I would like to thank John Skaritka for his help in obtaining the yoke section and other components, Tim Tuttle for his assistance in preparing the shims and assembling the cross section, and Mona Vitale for her help in making the measurements and punching the data onto computer cards. I would like to thank Dave Rahm and Steve Kahn for some useful suggestions.

TABLE I  
Iron Measurements

Half		$x_c$	$y_c$	R	$\chi^2$
AB	1	-0.0167	-0.0003	3.4173	221
	2	-0.0168	-0.0006	3.4167	187
	< >	-0.0167	-0.0004	3.417	
CD	1	-0.0032	-0.0072	3.4198	190
	2	-0.0036	-0.0077	3.4206	122
	< >	-0.0034	-0.0075	3.420	

TABLE II  
Pole Pieces

	Quad	$\alpha$	$\Delta\alpha$	b (mils)
inner	A	$4.17 \pm 0.01^\circ$	-0.01	$246 \pm 5$
	B	4.20	+0.02	$235 \pm 13$
	C	4.09	-0.09	$255 \pm 5$
	D	4.24	+0.06	$251 \pm 2$
	design	4.18		250
outer	A	39.68	+0.11	$233 \pm 19$
	B	39.65	+0.08	$246 \pm 17$
	C	39.58	+0.01	$230 \pm 4$
	D	39.63	+0.06	$238 \pm 4$
	design	39.57		250

TABLE III  
G-10 SHIMS

		Pre-assembly Thickness (mils)	Angular Size	Radius (inches)	Mean Thickness (mils)
inner	A	268 ± 1	5.534°	2.747	265
	B	256	5.164	2.747	248
	C	270	5.530	2.750	265
	D	271	5.549	2.750	266
outer	A	272	5.021	3.063	268
	B	272	5.022	3.063	268
	C	268	5.002	3.066	268
	D	268	4.933	3.066	264

TABLE IV  
Copper Wedges

		Angular size	Radius (inches)	Mean Thickness (mils)
inner	A	4.639°	2.747	222
	B	4.612	2.747	221
	C	4.621	2.750	222
	D	4.634	2.750	222
	design	4.62		
outer	A	4.913	3.063	263
	B	5.081	3.063	272
	C	4.982	3.066	267
	D	5.043	3.066	270
	design	4.97		

TABLE V  
Coil Segments

		N		Radius (inches)	t (mils)
inner	A	62	70.903	2.743	54.75
		4	4.724	2.747	56.62
	B	62	71.074	2.743	54.88
		4	4.635	2.747	55.56
	C	62	71.109	2.746	54.97
		4	4.747	2.750	56.96
	D	62	70.870	2.746	54.78
		4	4.593	2.750	55.11
outer	A	28	28.901	3.063	55.18
		11	11.444	3.063	55.62
	B	28	28.928	3.063	55.23
		11	11.355	3.063	55.18
	C	28	28.895	3.066	55.22
		11	11.339	3.066	55.16
	D	28	28.925	3.066	55.28
		11	11.353	3.066	55.23

TABLE VI  
Systematic Multipole Changes

n	Room Temp. <sup>2</sup> Design	Iron 45° Deformation	Outer Post Angle	Coil Radii	Inner Coil Friction
0	15.6039	-0.0014	+0.0020	+ .0152 <del>-0.0175</del>	-0.0004
2	-17.94	+0.52	+1.79	+ 2.03 <del>-4.39</del>	+3.31
4	6.62	+0.11	+0.26	- 1.13 <del>-1.47</del>	+2.98
6	0.50	-0.04	-0.08	- .33 <del>-0.40</del>	-0.22
8	-0.54	-0.01	0.00	+ .25 <del>+0.28</del>	-0.37
10	0.32	+0.01	+0.02	+0.02 ✓	+0.06

<sup>2</sup> H. Hahn & R. Fernow, ISABELLE Technical Note No. <sup>3</sup> 37 (1981) with  $R_{Fe} = 8.678$  cm.

TABLE VII  
Random Multipole Changes

n	Iron Radius Mismatch		Pole Piece Asymmetry	
	$b'_n$	$a'_n$	$b'_n$	$a'_n$
0	-0.0060		+0.0002	-6.64
1		-2.70	-3.52	0.00
2	-0.14		+0.10	+0.04
3		-0.51	-0.04	0.00
4	+0.02		0.00	-0.02
5		-0.08	-0.03	0.00
6	0.00		+0.01	0.00
7		-0.01	+0.01	0.00
8	0.00		0.00	0.00

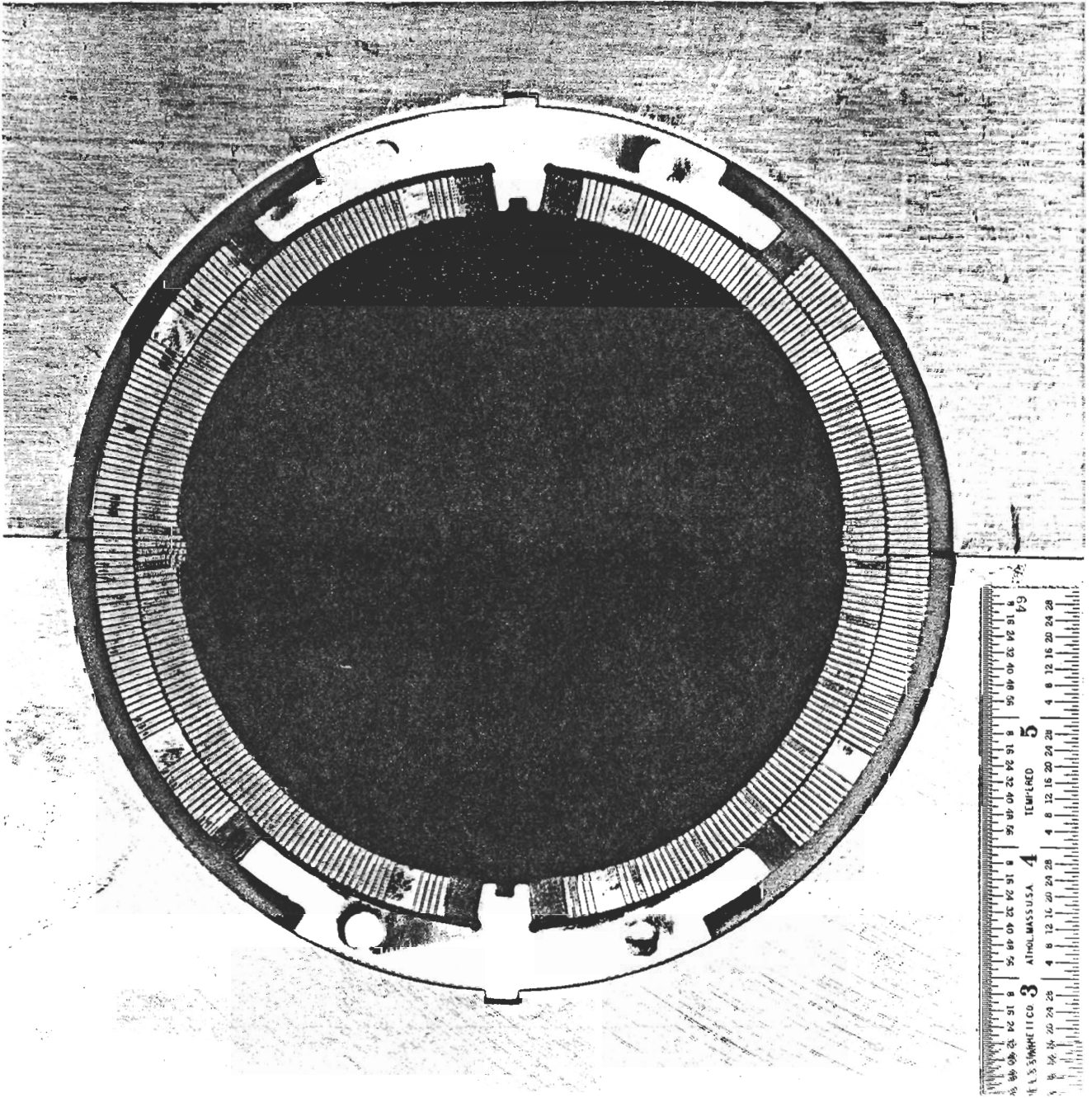


Figure 1

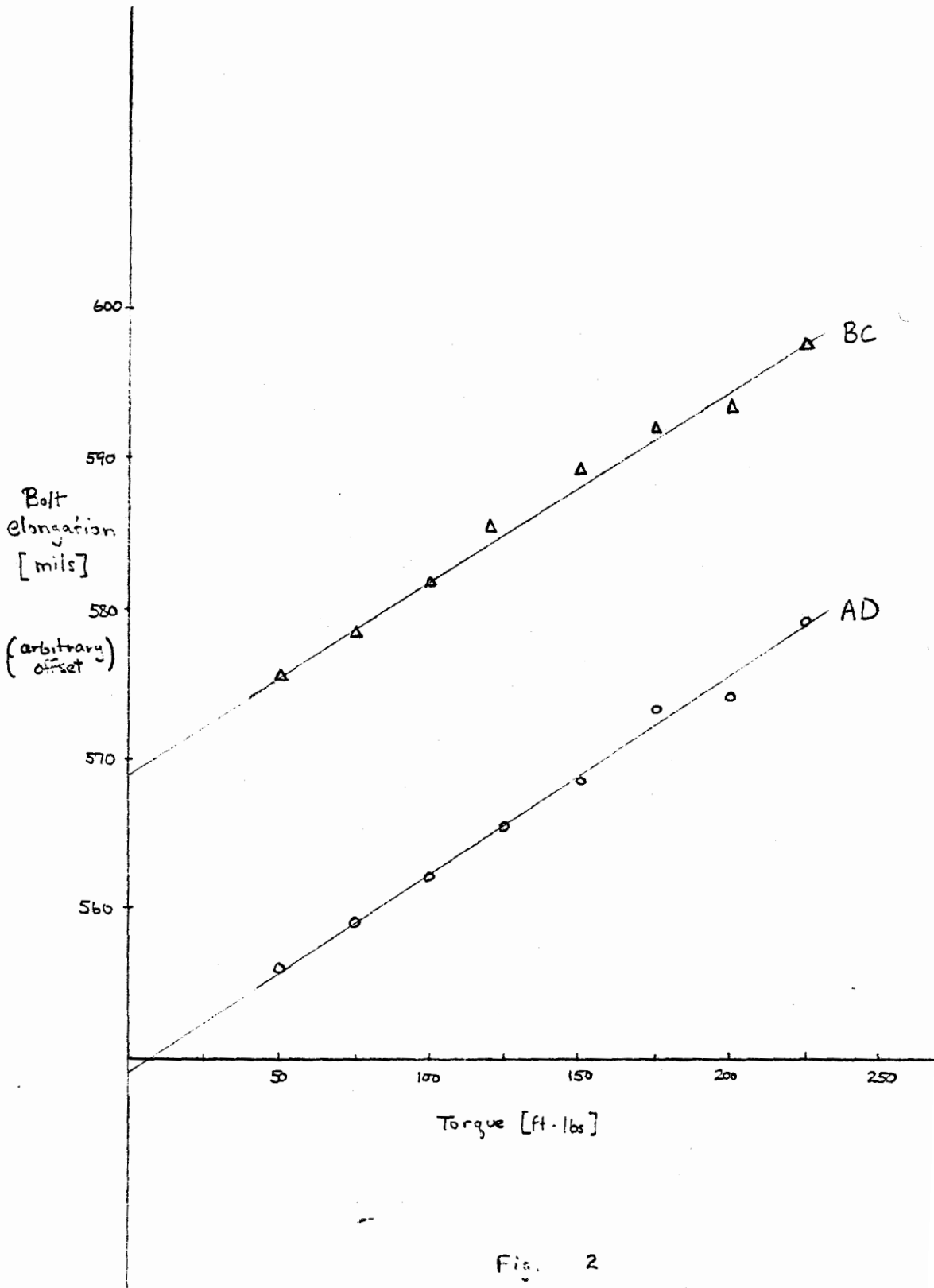


Fig. 2

30°  
330°

20°  
340°

10°  
350°

- 15 -  
○

350°  
10°

340°  
20°

330°  
30°

40°  
320°

50°  
310°

60°  
300°

70°  
290°

80°  
280°

90°  
270°

100°  
260°

110°  
250°

120°  
240°

130°  
230°

140°  
220°

320°  
40°

310°  
50°

300°  
60°

290°  
70°

280°  
80°

270°  
90°

260°  
100°

250°  
110°

240°  
120°

230°  
130°

220°  
140°

EUGENE DIETZGEN CO.  
MADE IN U. S. A.

NO. 341-P DIETZGEN GRAPH PAPER  
POLAR CO-ORDINATE

150°  
210°

160°  
200°

170°  
190°

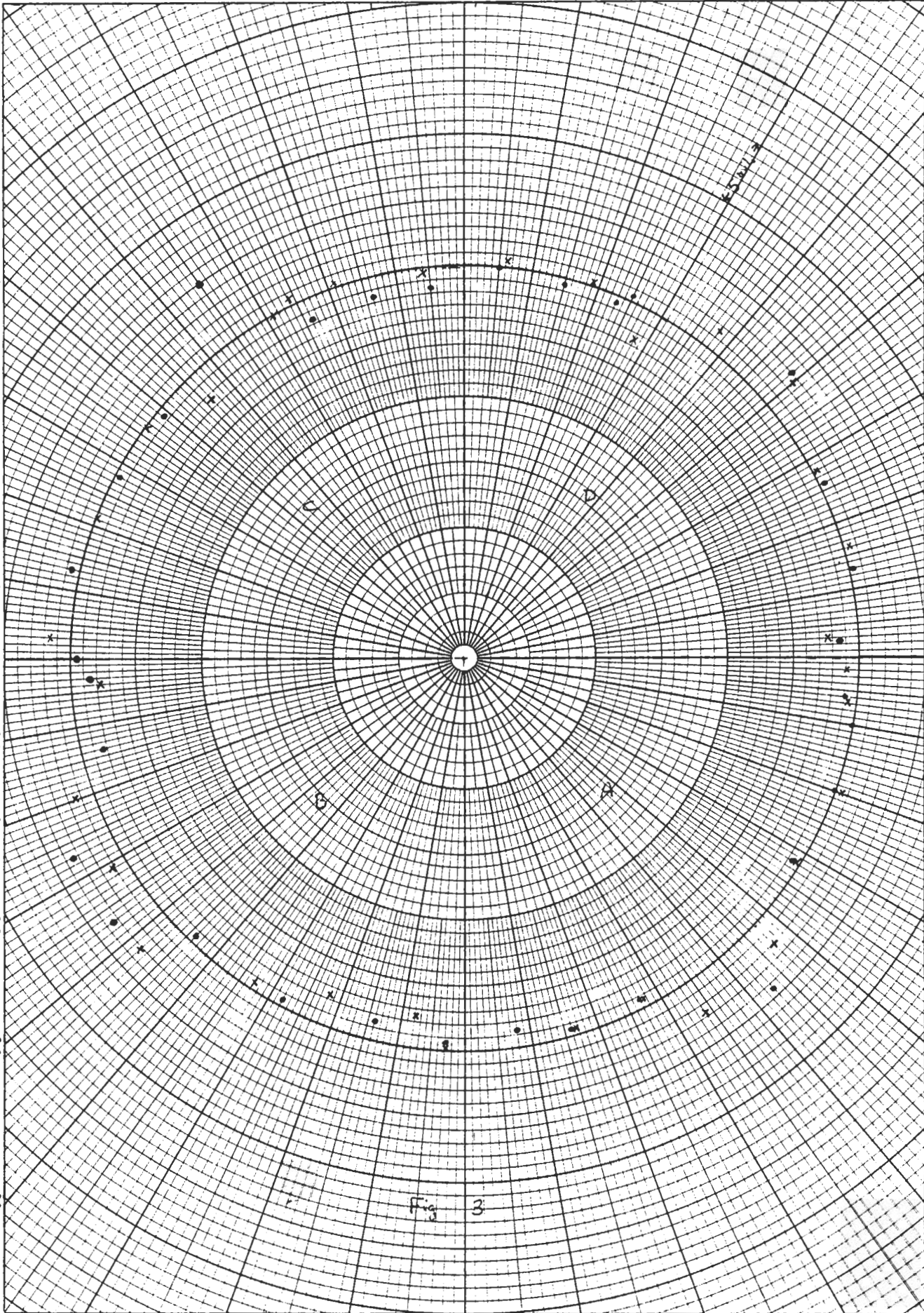
180°  
180°

190°  
170°

200°  
160°

210°  
150°

Fig 3



BY..... DATE.....

SUBJECT.....-16.....

SHEET No.....OF.....

CHKD. BY..... DATE.....

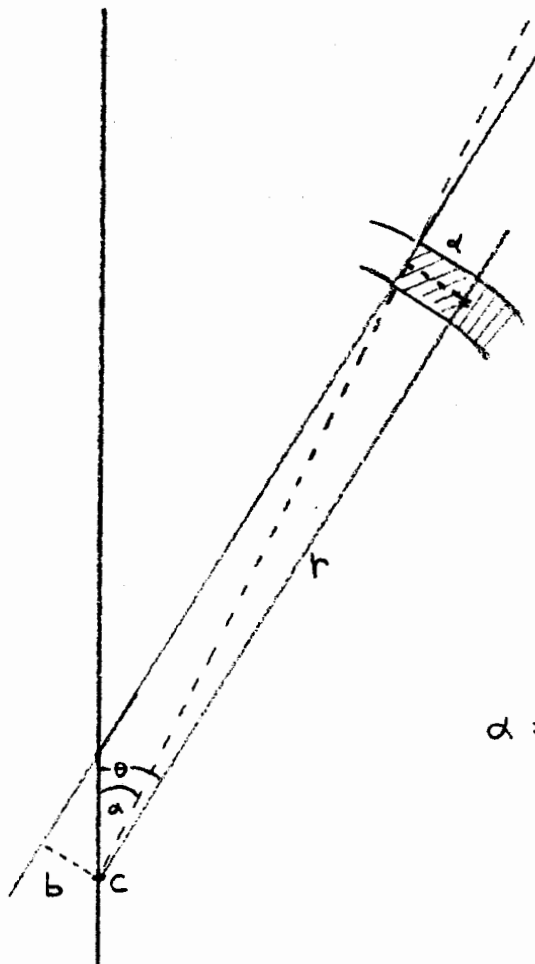
.....

JOB No.....

.....

DEPT. OR PROJECT.....

.....



$d$  = shim thickness

$\theta$  = design post angle

$\alpha$  = effective post angle

$r$  = mean coil radius

$$\alpha = \theta - \tan^{-1}\left(\frac{d}{r}\right)$$

Fig 4

BY \_\_\_\_\_ DATE \_\_\_\_\_ SUBJECT \_\_\_\_\_  
 - 17 -  
 CHKD. BY \_\_\_\_\_ DATE \_\_\_\_\_  
 DEPT. OR PROJECT \_\_\_\_\_

SHEET NO. \_\_\_\_\_ OF \_\_\_\_\_  
 JOB No. \_\_\_\_\_

|| Assembly radii

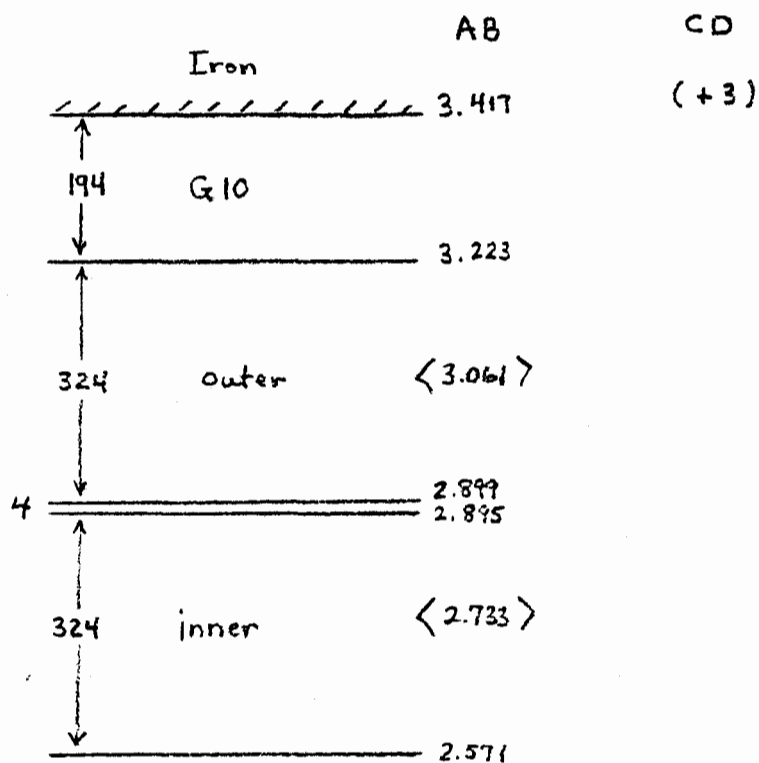


Fig 5

Outer coil bare conductor radii

C quadrant

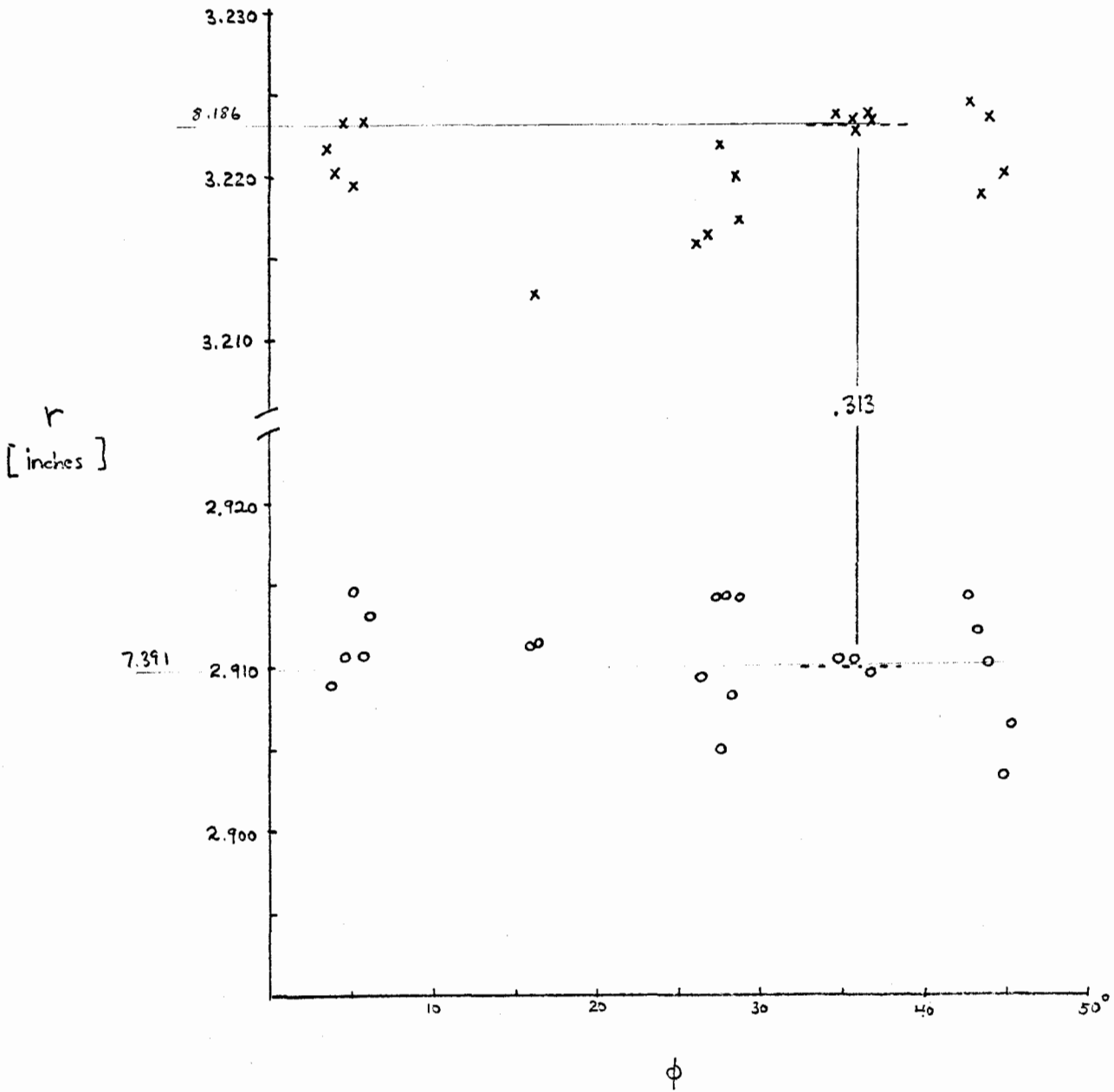


Fig 6

Inner coil bare conductor radii

C quadrant

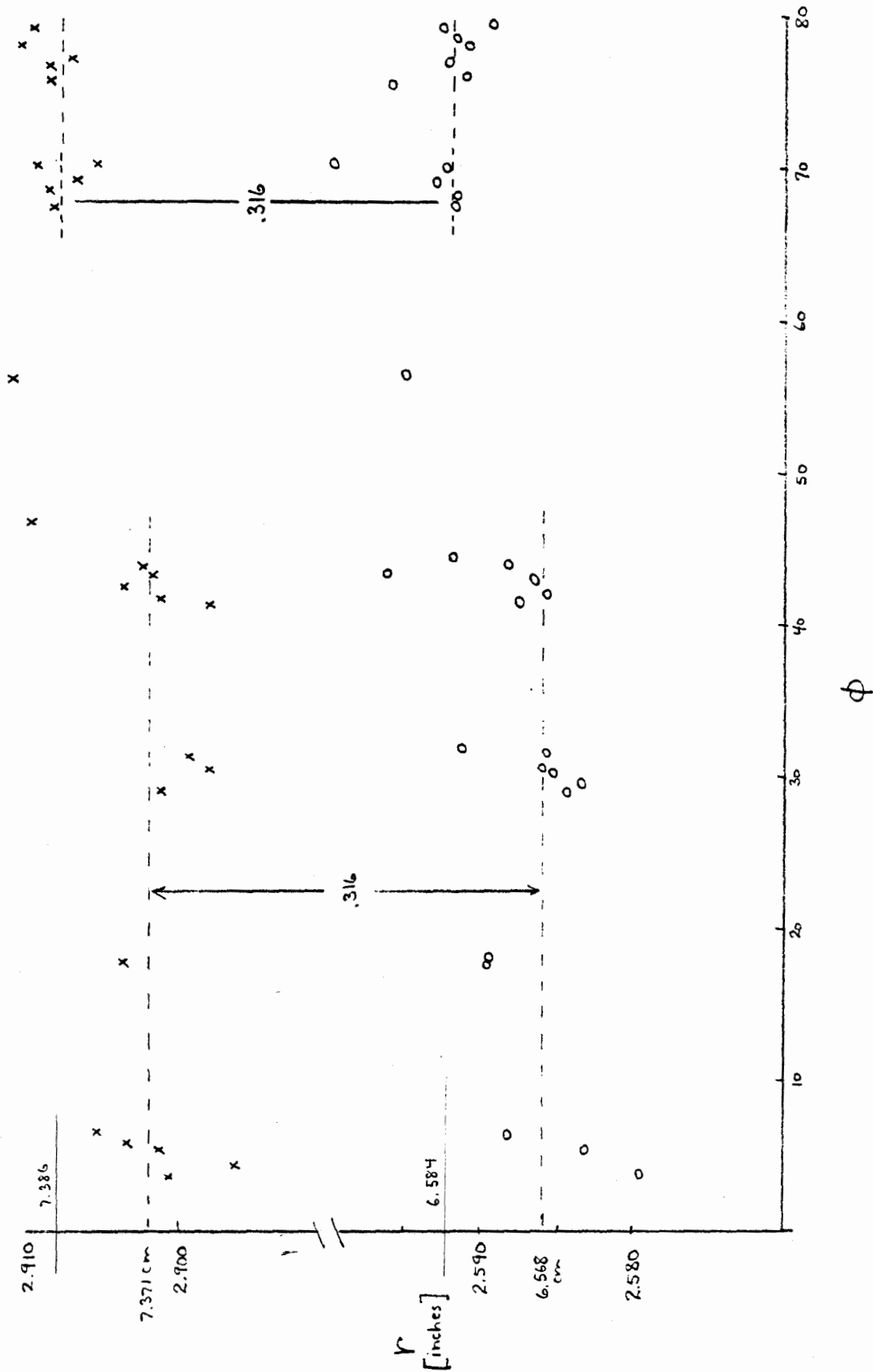


Fig 7

- A quadrant
- × C quadrant (edge 1)
- △ C quadrant (edge 2)

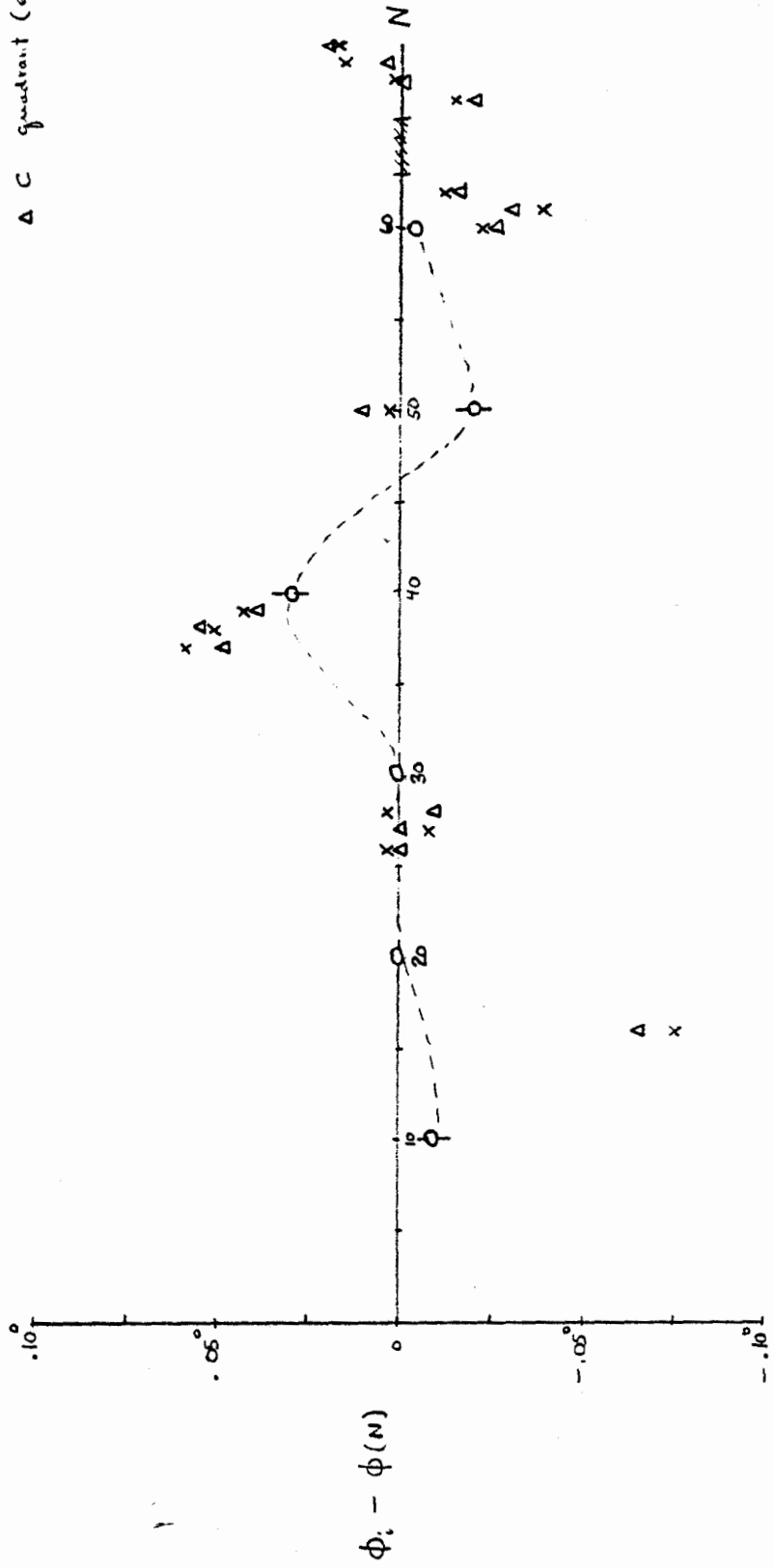
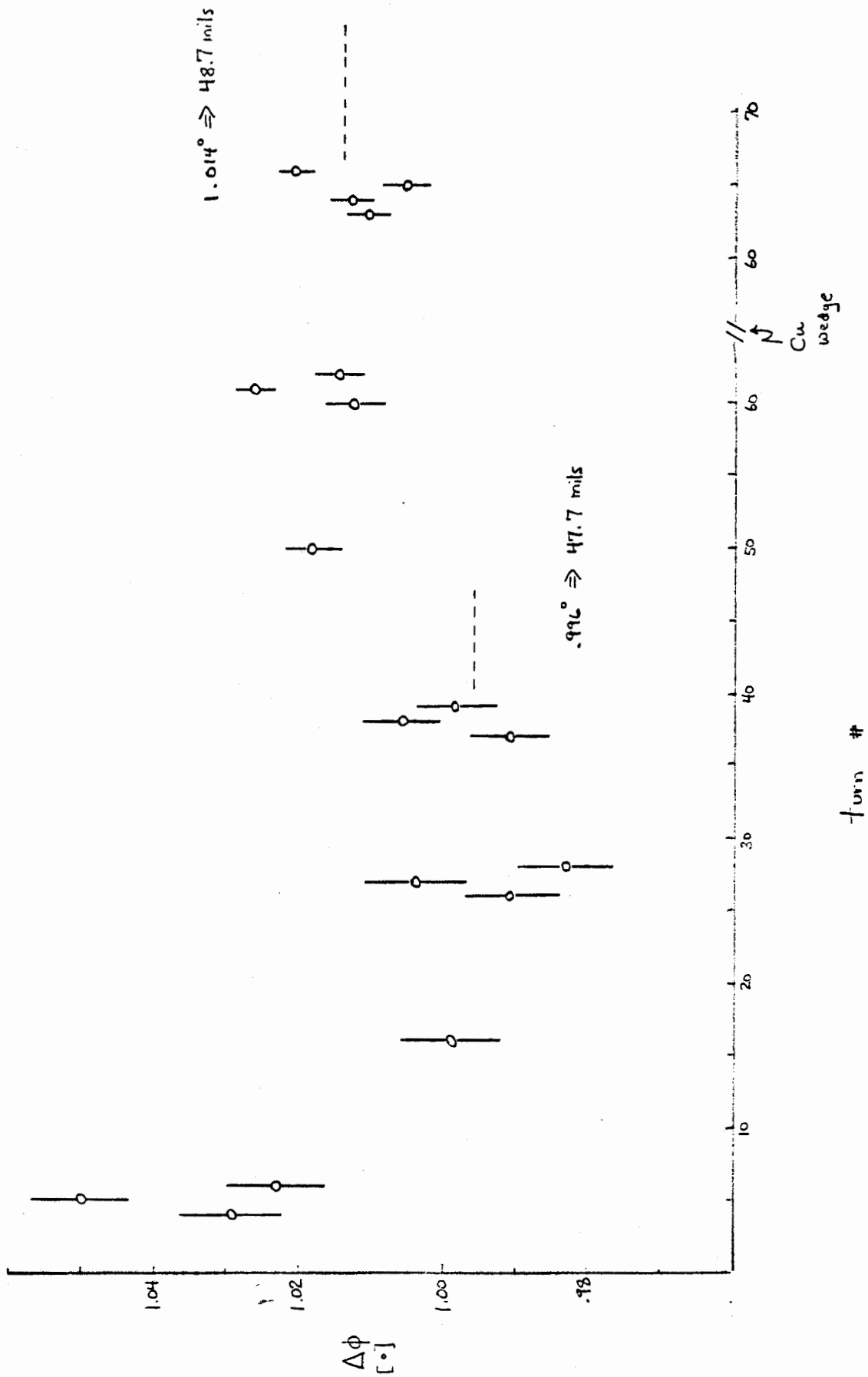


Fig. 8

Base conductor azimuthal thickness

C quadrant inner coil



Total azimuthal insulation between turns  
C quadrant inner coil

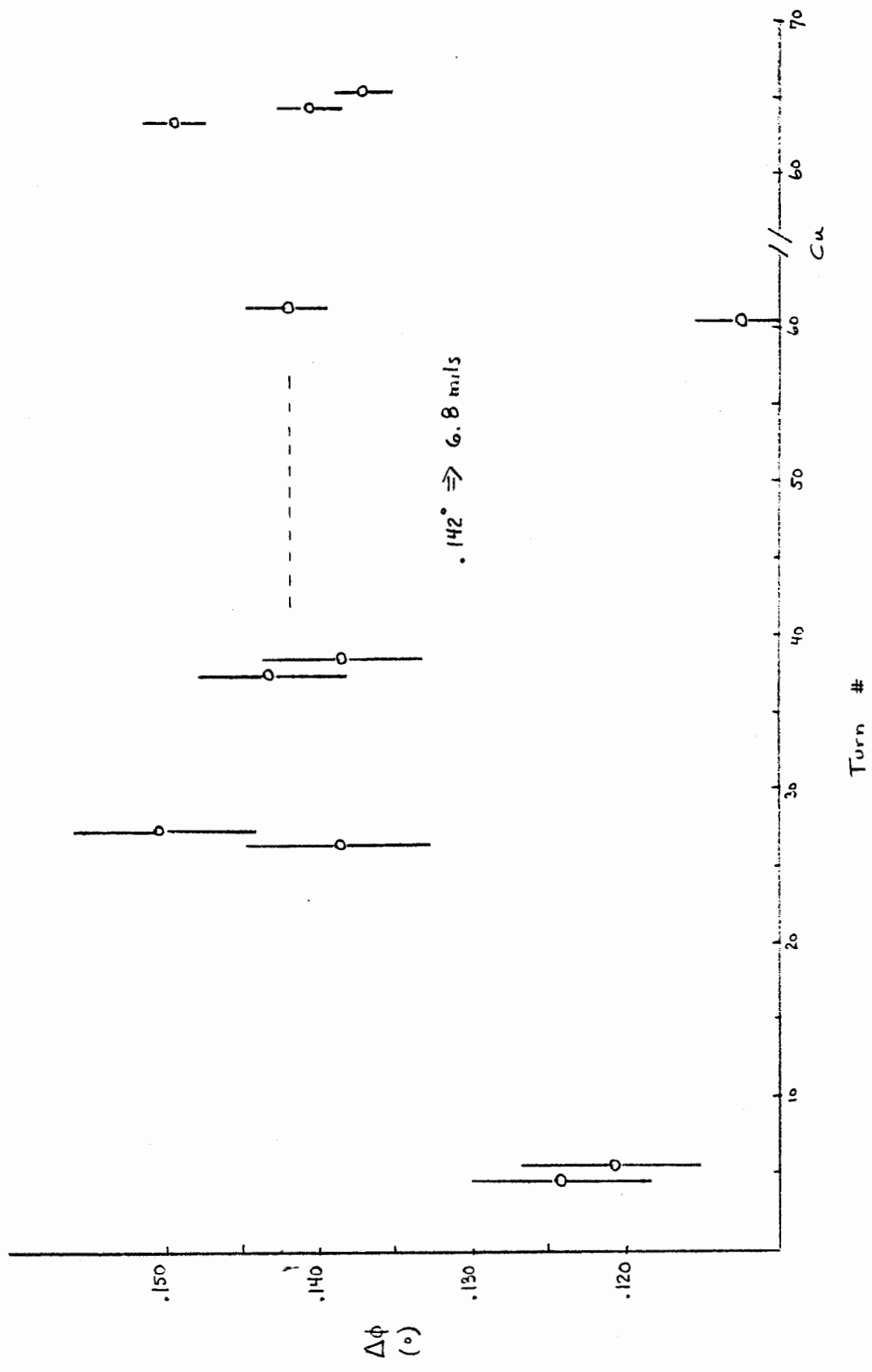


Fig 10

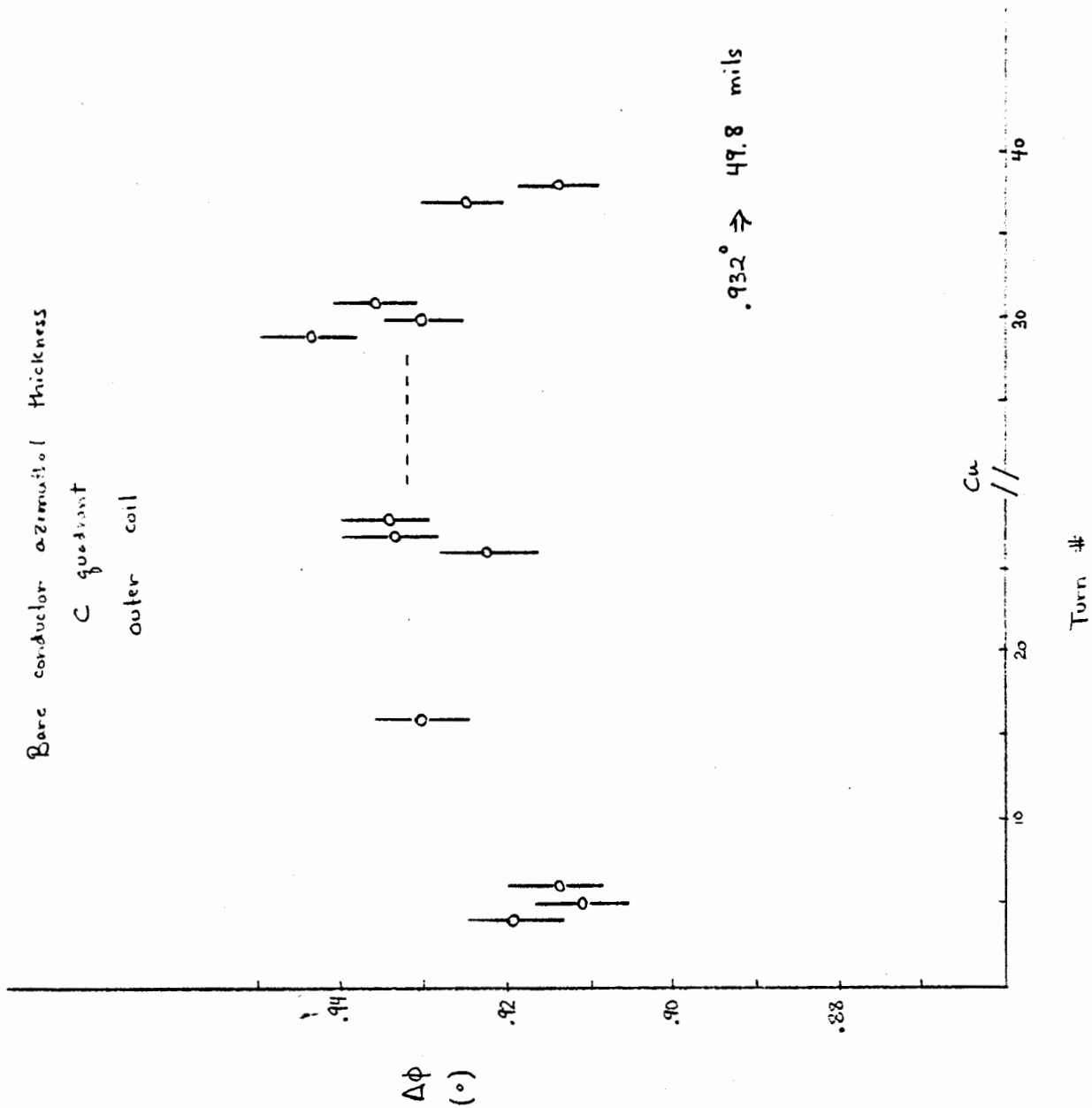


Fig 11

Total azimuthal insulation between turns

C quadrant  
outer coil

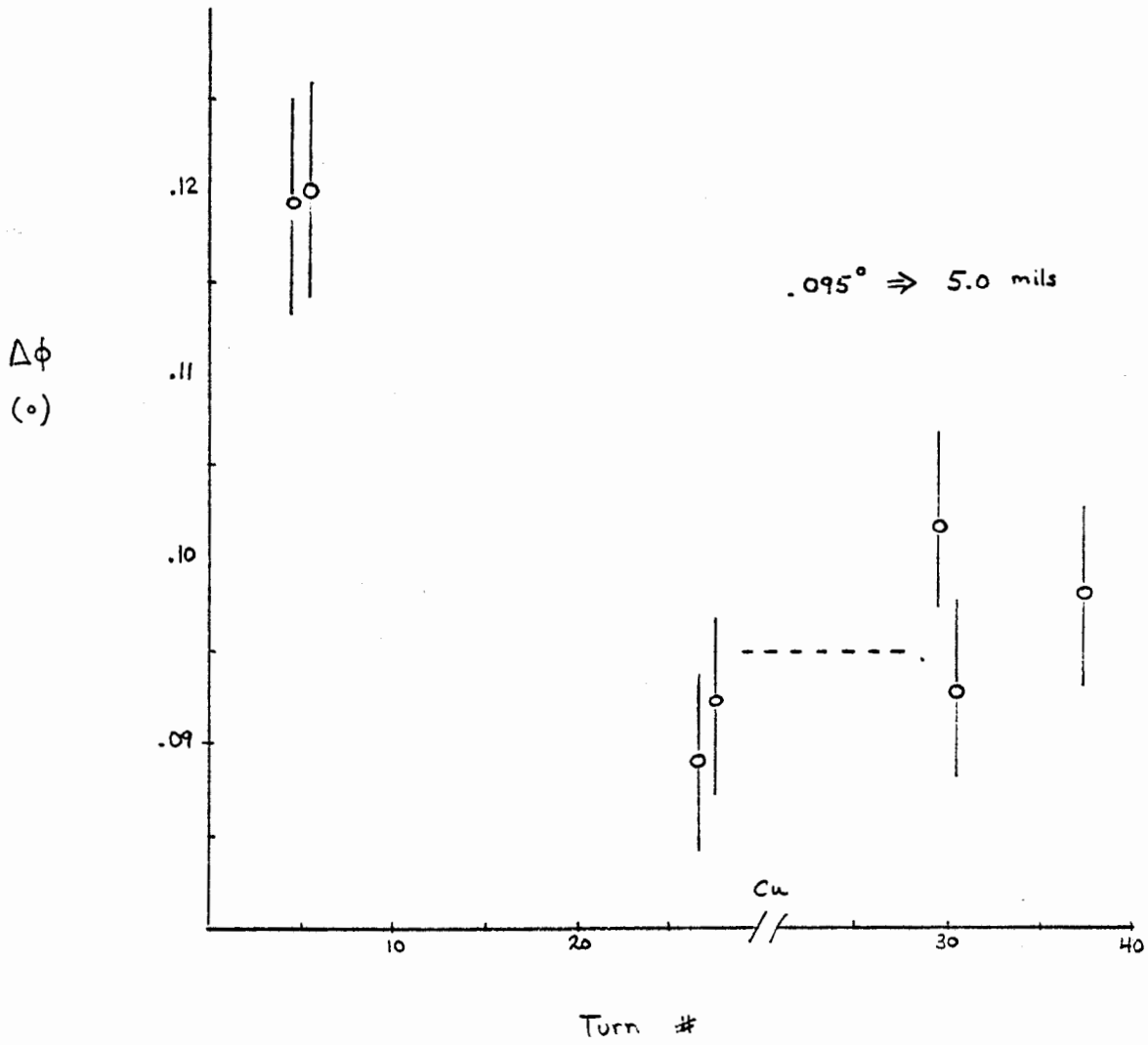
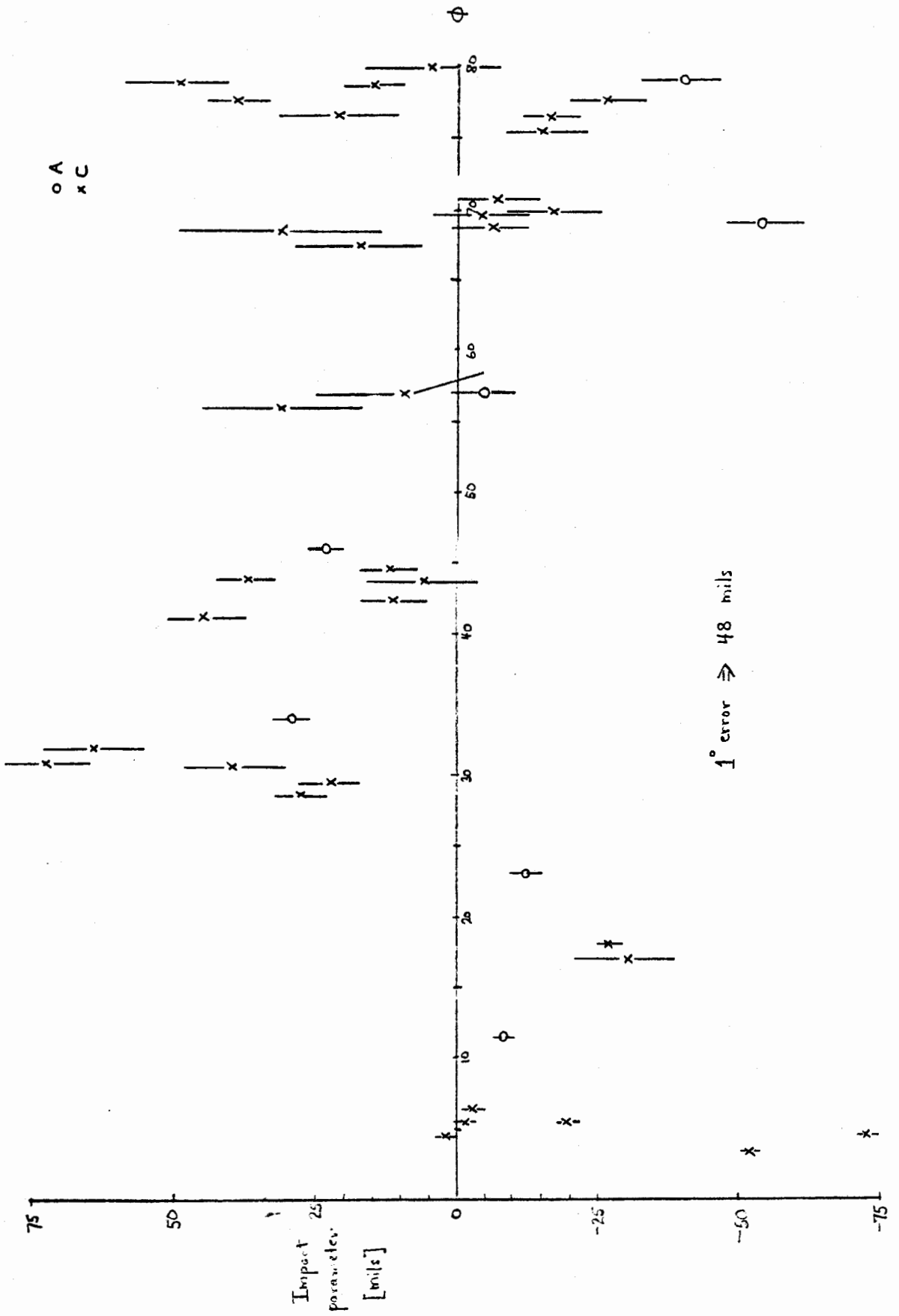


Fig 12

Impact parameters  
Inner coil



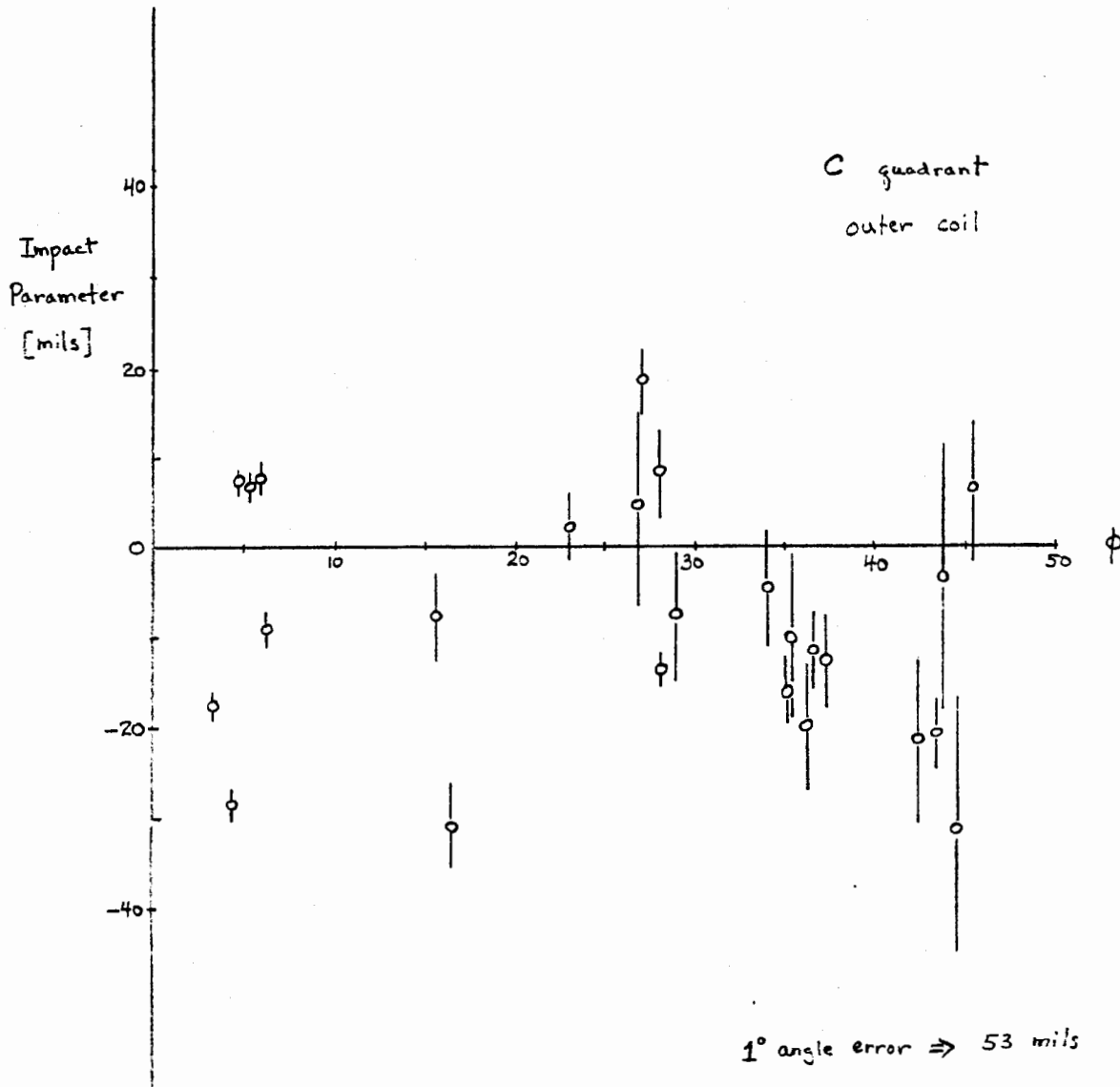
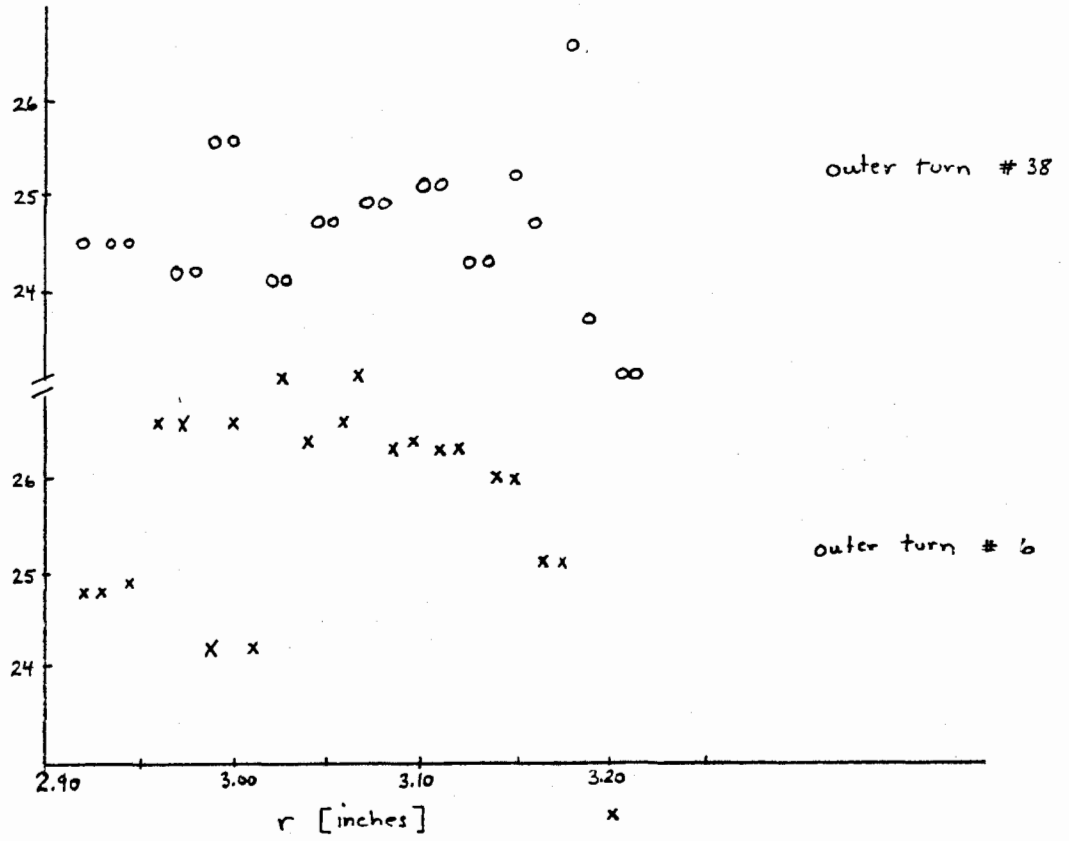


Fig 14

$d_{closest}$   
[mils]



$d_{closest}$   
[mils]

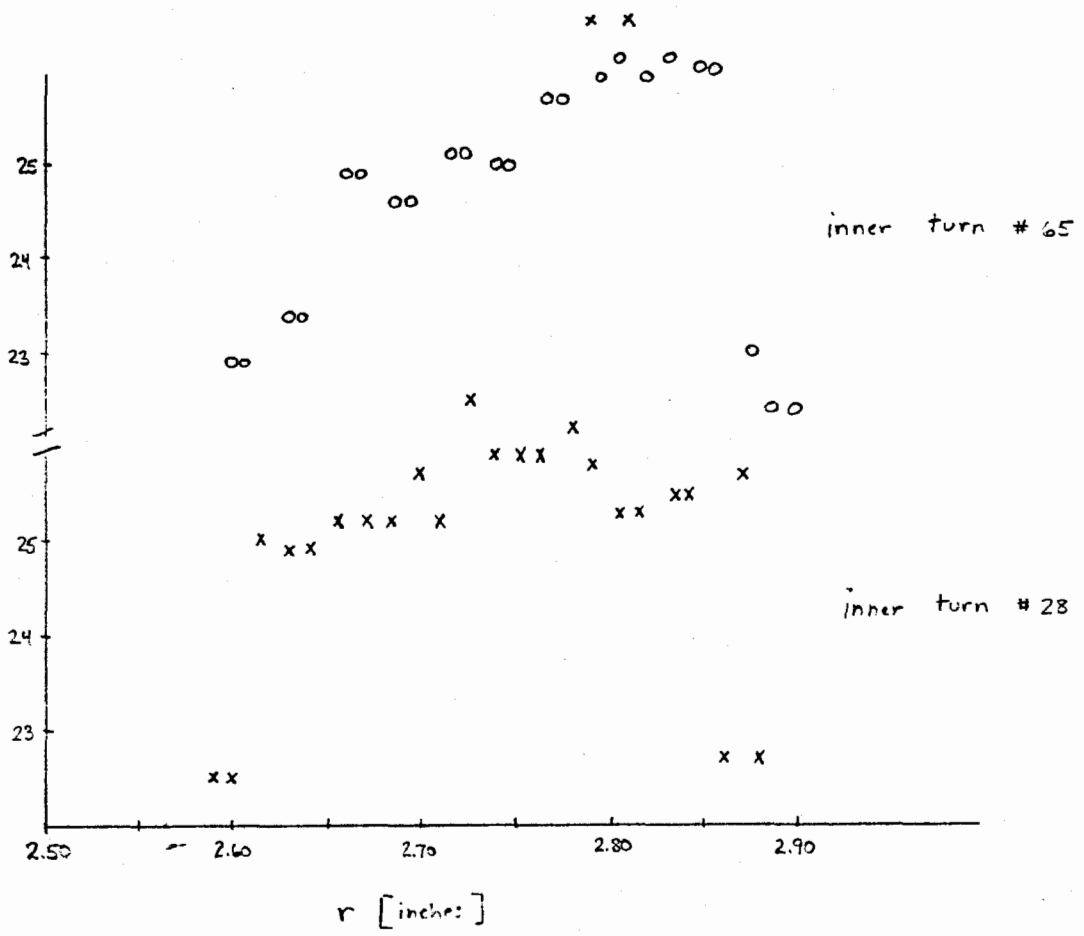


Fig 15

Bldg. 911

AD Library  
D. Lazarus  
D. Lowenstein  
M. Smith (1) plus  
one for each author(s) file  
J.R. Sanford  
D.H. White  
E. Jablonski

Bldg. 130

G. Bozoki

Bldg. 902

M.Q. Barton  
H. Foelsche  
H. Hahn  
H.J. Halama  
R.I. Louttit  
R.B. Palmer  
E.P. Rohrer  
N. Samios  
J. Spiro  
R.P. Shutt  
I. Stumer  
P. Tuttle

Bldg. 725

L. Blumberg for  
NSLS Library

Bldg. 510

H. Gordon  
T.F. Kycia  
L. Leipuner  
S. Lindenbaum  
S. Ozaki  
S. Protopopescu  
M. Sakitt  
T.L. Trueman  
  
W.R. Casey, 535A  
D.G. Dimmler, 535

R.R. Rau - MIT  
c/o S.C.C. Ting

Distribution: All Magnet Division Scientific and Professional Personnel (43).

/pmb